Cancer Screening and Prevention **2022** vol. 1(1) | 3–10
DOI: 10.14218/CSP.2022.00011

Original Article

Noninvasive Skin Cancer Screening Using Vibrational Optical Coherence Tomography: Differentiation Between Cancerous and Other Lesions Based on Mechanovibrational Testing

Frederick H. Silver[1,2*] and Tanmay Deshmukh[2]

[1]*Department of Pathology and Laboratory Medicine, Robert Wood Johnson Medical School, Rutgers, the State University of New Jersey, Piscataway, USA;* [2]*OptoVibronex, LLC., Bethlehem, Pennsylvania, USA*

Received: June 23, 2022 | **Revised:** August 24, 2022 | **Accepted:** September 06, 2022 | **Published:** November 04, 2022

Abstract

Background and objectives: In this study we use vibrational optical coherence tomography (VOCT) to study the mechanovibrational peak heights exhibited by benign and cancerous skin lesions. When a tissue is vibrated using audible sound it resonates at frequencies that represent the major components. The resonant frequency is related to the elastic modulus through a calibration equation developed *in vitro* using isolated tissue components. New cancerous skin lesions were identified based on the presence of a new cellular peak (80 Hz) with increased stiffness, a new blood vessel peak (130 Hz) that appears to be less stiff than normal blood vessels (150 Hz), and a fibrous tissue peak (260 Hz) present in carcinomas. The objective of this study was to differentiate different skin cancers using VOCT.

Methods: Mechanovibrational spectra were normalized by dividing by the largest peak of the different skin lesions. Differences in peak heights between actinic keratosis, basal cell carcinoma, squamous cell carcinoma, and melanoma were used to noninvasively "fingerprint" the different skin lesions.

Results: The results suggest that VOCT can be used to noninvasively differentiate between different skin cancers and to identify early skin cancers possibly as small as 0.1 mm based on the heights of the 50, 80, and 130 Hz peaks

Conclusions: Further work is underway to use machine learning in conjunction with quantitative VOCT peak heights derived from mechanovibrational spectra to noninvasively identify different skin cancers.

Introduction

Differentiation of normal skin from benign skin lesions and from cancerous tissue has been a major diagnostic challenge as the number of skin cancers continues to increase worldwide. Yet, early diagnosis of small lesions is important to provide a wider array of treatment options. Excisional versus topical treatments have become important issues especially for keratinocyte cancers. Depending on their size, shape, and rate of recurrence there may be different treatment options.[1,2] While identification of basal cell carcinoma can be easily achieved based on visual and dermoscopic analysis, identification of lesion subtype can be further refined based on other imaging methods including ultrasound and vibrational optical coherence tomography, based on their size and shape.[3,4]

We recently developed a technique termed vibrational optical coherence tomography (VOCT) to noninvasively characterize different types of skin cancers.[4–8] The results indicate that cancerous lesions are characterized by deposition of stiff fibrotic tissue, new

Keywords: Cancer; Screening; Fibrosis; Vibrational OCT; Stiffness; Vibrational analysis; Actinic keratosis; BCC; SCC; Melanoma.

Abbreviations: AK, actinic keratosis; BCC, basal cell carcinoma; CAF, cancer associated fibroblasts; COL(I), collagen type I; ECM, extracellular matrix; EMT, epithelial mesenchyme transition; SCC, squamous cell carcinoma; TGF-beta-1, transforming growth factor beta-1; VOCT, vibrational optical coherence tomography.

***Correspondence to:** Frederick H. Silver, Department of Pathology and Laboratory Medicine, Robert Wood Johnson Medical School, Rutgers, the State University of New Jersey, Piscataway, New Jersey 08854, USA. ORCID: https://orcid.org/0000-0002-2480-9264. Tel: 1-5708976544, Fax: +1-5708975444, E-mail: silverfr@rwjms.rutgers.edu

How to cite this article: Silver FH, Deshmukh T. Noninvasive Skin Cancer Screening Using Vibrational Optical Coherence Tomography: Differentiation Between Cancerous and Other Lesions Based on Mechanovibrational Testing. *Cancer Screen Prev* 2022;1(1):3–10. doi: 10.14218/CSP.2022.00011.

blood vessels, and new cancer associated cells that are not present in the papillary and reticular dermis of normal skin.[5–8] The finding of resonant frequency peaks consistent with the deposition of stiff fibrotic tissue is consistent with the reports that lysyl oxidase promotes crosslinking of stiff, highly collagenous tissue.[9–12] The presence of fibrous tissue demonstrated by VOCT measurements may provide a method for early screening of both skin and other epithelial cell-derived cancers.

Beyond its role in cancer, organ fibrosis affects all major human tissues and can lead to excessive accumulation of extracellular matrix (ECM) components, predominantly collagens. Forty-five percent of all deaths in the developed world are believed to be associated with fibrosis.[13] A clear relationship between chronic inflammation, fibrosis, and cancer dates back almost 200 years.[14] The ability to noninvasively detect tissue and organ fibrosis is an important tool to allow early diagnosis of many fibrotic diseases.

Cancer associated fibroblasts (CAFs), but not normal fibroblasts, support metastatic lesions.[15] CAFs and tumor cells are regulated by provisional matrix molecules, leading to continued stromal collagen cross-linking, and resulting fibrosis.[10] CAFs are major components of the stroma surrounding carcinomas. New cells, as well as new blood vessels, are seen in cancerous skin lesions. For example, in basal cell carcinoma (BCC) vessels are seen with large diameters that are branching as well as superficial vessels (telangiectasia) consisting of short fine linear vessels with fine branches.[16] While imaging methods can provide qualitative differences between normal blood vessels and cancer associated vasculature, VOCT can provide quantitative differences that can be used to differentiate benign from cancerous skin lesions.[4–8] Besides measuring tissue component stiffness using VOCT, it is possible to create a "virtual biopsy" mapping the location of new cells and fibrotic tissue.[6]

Both cancer cells and skin cancerous tissue are stiffer than normal tissue.[17–20] The increased stiffness of cancer associated cells and fibrous tissue found in skin carcinomas using VOCT has been reported previously.[4–8] The technique applies audible sound and infrared light transversely to the skin surface providing an image and a mechanovibrational spectrum of the major skin components.[4–8] Normal skin has major resonant frequency peaks at 50 Hz (stiffness about 1.2 MPa), 100 Hz (2.5 MPa), and 150 Hz (4.5 MPa), while cancerous lesions have new peaks at 80 Hz, 130 Hz, and 260 Hz.[4–8] The 50 Hz (1.2 MPa) peak appears to reflect the behavior of epidermal cells and fibroblasts, while the 150 Hz (4.5 MPa) peak is like that seen in normal arteries and veins.[21] The new peaks at 80 Hz (about 2.1 MPa) and 130 Hz (about 4.5 MPa) have been hypothesized to reflect the presence of new pre-cancerous and other cells (perhaps CAFs) that are associated with new blood friable blood vessels (130 Hz peak). The 260 Hz peak observed in all cancerous skin lesions is associated with the formation of fibrous tissue (about 16 MPa) and is much higher than the modulus of dermal collagen (about 2.5 MPa).[4–8] By creating a vibrational spectrum of each skin lesion type, it is possible to develop a lesion fingerprint that can be used to noninvasively provide an early diagnosis of lesions as small as about 0.1 mm in diameter.

The purpose of this study was to compare the mechanovibrational peaks found in normal skin, actinic keratosis (AK), BCC, squamous cell carcinoma (SCC), and melanoma to identify differences that can be used to create a "fingerprint" of each type of skin lesion as an early screening test for skin cancer. These "fingerprints" may be used with machine learning algorithms to identify lesions that have metastatic potential before they grow in size. In addition, the ability to define the interface between normal skin and cancerous tissue noninvasively would facilitate complete lesion removal during surgery. The results reported in this study suggest that the mechanovibrational peaks observed by vibrational optical coherence tomography can provide a specific lesion "fingerprint" that can be used to noninvasively screen different skin carcinomas. The differences in the resonant frequency peak locations can potentially be used to locate the boundaries of cancerous tissues.

Methods

Subjects

Normal skin from 14 subjects (11 males and 3 females) was studied *in vivo* using VOCT after informed consent was obtained as reported previously.[22] Resonant frequencies of the components of skin were measured *in vivo*.[22] The subjects ranged in age from 21 to 71 years old. Previous VOCT study results suggest that the frequencies of mechanovibrational peaks are similar when measured either *in vitro* or *in vivo*.[7]

Lesions identified by dermoscopy in the Dermatology Clinic at Summit Health (Berkeley Heights, NJ) were biopsied and studied *in vitro* as previously reported.[22] The biopsied lesions were studied blindly by VOCT *in vitro* without identification of the age and sex of the patient. All subjects signed consent forms prior to enrolling in the study. Pathologic diagnoses were compared to mechanovibrational peak heights observed by VOCT after correction for speaker vibrations and vibrations not in phase with the input sinusoidal sound wave.[22]

OCT images

OCT image collection was accomplished using a Lumedica Spectral Domain OQ 2.0 Labscope (Lumedica Inc., Durham, NC) as described previously and was correlated with the histological images seen in sections cut from tissue biopsies as reported elsewhere.[4–8]

Measurement of resonant frequency and elastic modulus

The OQ Labscope was modified by adding a 2-inch diameter speaker to vibrate the tissue in the VOCT studies and modified to collect and store single raw image data that was used to calculate sample displacements (amplitude information) from amplitude line data.[4–8,21] The vibrations for each frequency were isolated to calculate the amplitude. These amplitudes were plotted against the frequency of the vibrations. Mechanovibrational spectra of all samples were normalized by dividing by the height of the largest peak.

The measured resonant frequencies were converted into elastic modulus values using a calibration equation (Equation 1).[4–8] The peak frequency (the resonant frequency), f_n is related to the elastic modulus, E in MPa and the sample thickness d in meters.

$$\text{Soft Tissues} \qquad E \times d = 0.0651 \times (fn) + 233.16 \qquad (1)$$

Modulus values listed in Table 1 were calculated using Equation (1).

Normal skin studies were conducted *in vivo* using a universal hand piece mount.[22] Once VOCT studies were conducted, the biopsy samples were processed and reviewed by a trained Mohs dermatopathologist who conducted the pathological analysis.

Results

Results of experiments conducted on normal skin *in vivo* and excisions of AK, BCC, SCC, and melanoma *in vitro* indicate that

Table 1. Resonant frequencies and moduli of normal skin, AK, BCC, SCC, and melanoma were studied

		Resonant Frequency				
Sample	**No. of Measurements**	**50 Hz**	**80 Hz**	**100 Hz**	**130 Hz**	**260 Hz**
Normal Skin	14	50 {0}	NA	100 {0}	NA	NA
AK	7	50 {0}	75.71 {7.68}	104.28 {5.34}	127.14 {4.81}	NA
Nodular BCC	27	52.77 {4.60}	75.55 {5.06}	102.22 {4.23}	125.18 {5.09}	262.59 {4.46}
Superficial BCC	6	54 {5.47}	80 {0}	102 {4.47}	126.67 {5.16}	261.67 {4.08}
SCC	46	49.56 {2.06}	75.86 {4.97}	104.78 {5.05}	127.82 {4.17}	262.82 {4.55}
Melanoma	57	50 {0}	76.31 {4.86}	102.20 {4.18}	128.24 {3.83}	262.98 {4.61}
Normal Skin	14	1.231 {0.140}	NA	2.66 {0.32}	NA	NA
AK	7	0.88 {0.160}	1.60 {0.24}	2.54 {0.81}	4.52 {1.206}	NA
Nodular BCC	27	1.467 {0.26}	2.31 {0.41}	3.20 {0.46}	4.41 {0.78}	16.51 {2.65}
Superficial BCC	6	1.525 {0.74}	2.27 {0.40}	2.86 {1.207}	4.46 {0.69}	16.38 {2.82}
SCC	46	1.304 {0.156}	2.02 {0.28}	3.15 {0.45}	4.30 {0.47}	15.68 {1.826}
Melanoma	57	1.459 {0.162}	2.26 {0.29}	3.36 {0.41}	4.81 {0.56}	17.44 {1.938}

All values are in MPa. N is the number of measurements made for each lesion, and the standard deviation is shown in parentheses after the mean value of each measurement. Note that all measurements were made at 10 Hz intervals. The values of modulus are listed in the lower part of the table.

there is a relationship between the organization of new cells at (80 Hz), new blood vessels (130 Hz), and fibrous tissue (260 Hz) in benign and cancerous lesions. Differences in the peak heights and frequencies can be used to differentiate among normal skin, AK, BCC, SCC, and melanoma based on the data shown in Figures 1–7 and Tables 2 and 3.

Figure 1 shows a normalized mechanovibrational spectrum of normal skin as well as a cross-sectional OCT image of a typical area of normal skin. Data were normalized by dividing by the peaks due to the speaker and then by the highest peak in the spectrum. Note the peaks at about 50 Hz (cells), 100 Hz (dermal collagen), and 150 Hz (blood vessels) are typical of what is found in normal skin as reported previously.[4–8]

Figure 2 shows a normalized mechanovibrational spectrum of an AK (a), as well as an OCT image of the cross-section of the AK (b) where the measurements were made. The peaks at about 50 Hz (cells), 100 Hz (dermal collagen), and 150 Hz (blood vessels) are those found in normal skin. New peaks at 80 Hz and 130 Hz are found in AKs.

Figure 3 shows a normalized mechanovibrational spectrum of a typical nodular BCC (a), as well as an OCT image of the cross-section (b). Note the new peaks at about 80 Hz (cells) and 130 Hz (blood vessels) are similar to those found in AK and are supplemented by a new peak at 260 Hz that is not typically found in AK or normal skin.

Figure 1 illustrates that normal skin has prominent peaks at 50

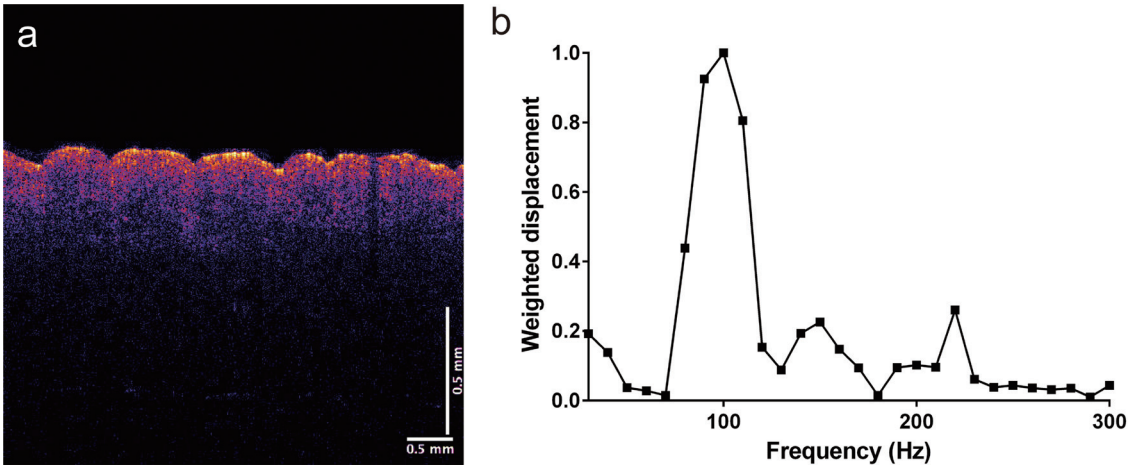

Fig. 1. OCT image and VOCT spectrum for normal skin. (a) 2D color coded OCT image of a cross-section of normal skin. (b) Plot of weighted displacement versus frequency for normal skin. The weighted displacement is calculated by dividing the displacement of the sample by the displacement in the absence of the sample by the speaker. Note the peaks at about 50 Hz (cells), 100 Hz (dermal collagen), and 150 Hz (blood vessels) are found in normal skin. The cells are found primarily in the epidermis and papillary dermis, while the dermal collagen and blood vessels are found in the papillary dermis. The color coding was accomplished by using the pixel intensity and a look-table to assign the colors.

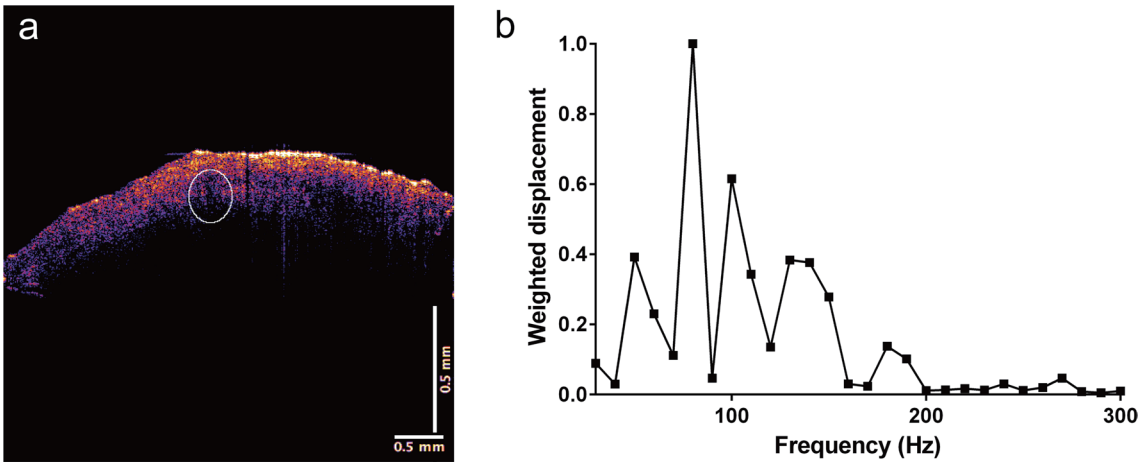

Fig. 2. OCT image and VOCT spectrum for an actinic keratosis. (a) 2D color coded OCT image of a cross-section an actinic keratosis (AK). The area where the lesion is present is shown in the circle. (b) A 2D plot of weighted displacement versus frequency showing the mechanovibrational peaks of new lesions cells (80 Hz), new lesion associated blood vessels (150 Hz), papillary collagen (100 Hz), and blood vessels (150 Hz). Note the peaks at 80 Hz and 130 Hz are not seen in normal skin. The color coding was accomplished by using the pixel intensity and a look-table to assign the colors.

Hz, 100 Hz, and 150 Hz, while AK has additional at peaks at 80 Hz and 130 Hz. Normal skin and AKs have different distributions of peak heights from BCCs, SCCs, and melanomas. AK has peaks at 80 Hz and 130 Hz, which distinguishes its profile from normal skin. It lacks a peak at 260 Hz, which differentiates AK from BCC, SCC, and melanoma (see Figs. 3–5).

Figure 4 shows a normalized mechanovibrational spectrum of a typical SCC (a), as well as an OCT image of the cross-section where the measurements were made (b). As shown in Tables 2 and 3, the peak height ratios for SCC are statistically different from those seen in BCC and melanoma.

Figure 5 shows a normalized mechanovibrational spectrum of a typical melanoma (a) and OCT images (b) of the cross-section of a melanoma where the measurements were made. Melanoma has different peak heights than are observed for BCC and SCC. As seen in the data shown in Tables 2 and 3, melanoma has peak height ratios that are statistically different when compared to BCC and SCC.

Figure 6 compares the normalized peak heights (normalized by dividing by the largest peak in a mechanovibrational spectrum of each sample) for normal skin, AK, BCC, SCC, and melanoma along with the standard deviations shown as error bars above the peaks. Peak locations, peak height differences, and peak height ratios can be used to differentiate differences in normal skin, AK, BCC, SCC, and melanoma as shown in Figures 6 and 7, as well as based on the data in Tables 2 and 3.

Figure 7 (a) shows the ratio of the 50 Hz and 80 Hz peak heights for BCC, SCC, and melanoma. The increased 50 Hz/80 Hz peak height ratio is significantly different for SCC compared to melanoma and BCC at a confidence level greater than 0.95, as shown in Table 2. Figure 7 (b) shows the relationship between the 130 Hz/80 Hz peak height ratios for BCC, SCC, and melanoma. The peak height ratio for melanoma is significantly different at a confidence level greater than 0.95 for BCC and SCC as indicated in Table 3.

Table 1 compares the stiffness of each peak shown in Figure 6,

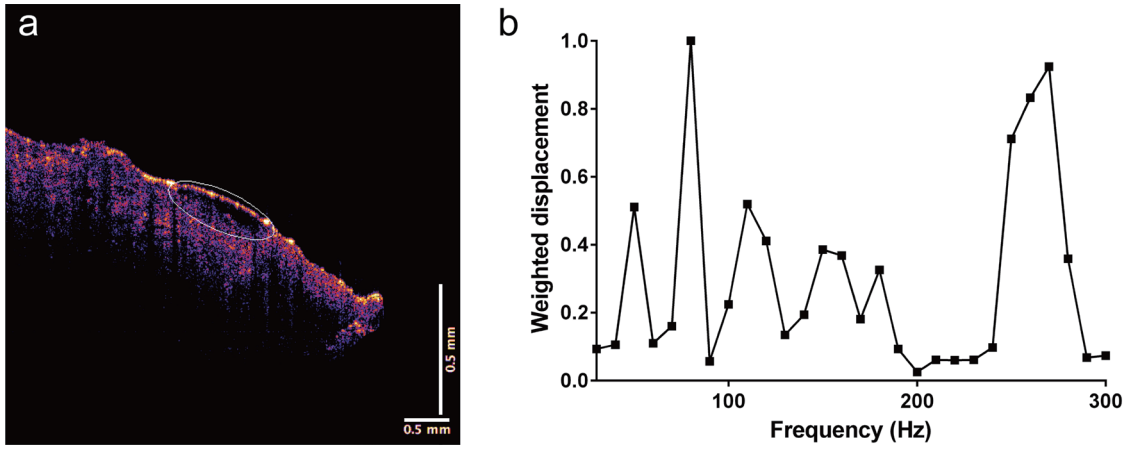

Fig. 3. OCT image and a VOCT spectrum for a basal cell carcinoma. (a) 2D color coded OCT cross-sectional image of a nodular basal cell carcinoma (BCC). (b) 2D plot of weighted displacement versus frequency showing the peaks from skin cells (50 Hz), new cells (80 Hz), dermal collagen (100 Hz), and fibrotic tissue (260 Hz) for a nodular BCC. Note the presence of 80 Hz, 130 Hz, and 260 Hz peaks are indicative of cancerous tissue. The color coding was accomplished by using the pixel intensity and a look-table to assign the colors.

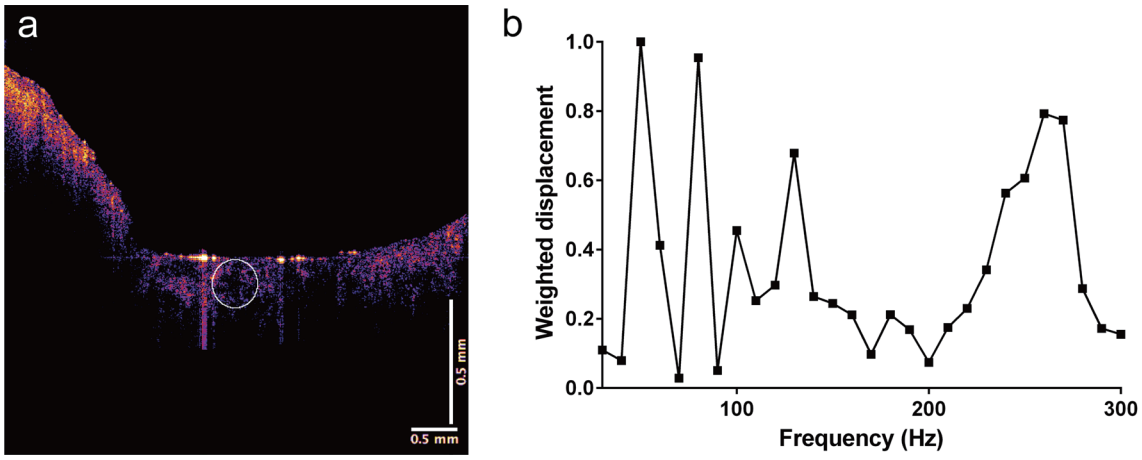

Fig. 4. OCT image and a VOCT spectrum for a squamous cell carcinoma. (a) 2D color coded cross-sectional OCT image of a squamous cell carcinoma (SCC) that is circled. (b) 2D plot of weighted displacement versus frequency showing the peaks from skin cells (50 Hz), new cells (80 Hz), papillary collagen (100 Hz), new blood vessels (130 Hz), and fibrotic tissue (260 Hz). Note the increased size of the peak at about 50 Hz and a large 260 Hz peak that are a characteristic of SCC as opposed to melanoma and BCC. The color coding was accomplished by using the pixel intensity and a look-table to assign the colors.

illustrating that the new cells at 80 Hz are stiffer than normal skin cells (50 Hz), and that fibrous tissue in cancerous lesions (260 Hz) is much stiffer than normal dermal collagen (100 Hz).

Discussion

A new technique termed VOCT, can be used to screen skin cancers noninvasively based on the morphology and stiffness of the lesions. The addition of new cells with increased stiffness (80 Hz), new blood vessels (130 Hz), and stiff fibrous tissue (260 Hz) that are present in all carcinomas studied can be used to differentiate benign from cancerous skin lesions.[4–8,20–22] These results suggest that the product of fibrosis that results from cellular mutation is similar for different types of skin cancers, including cancers that have invasive and metastatic potential. While BBCs form primarily localized lesions, other cancers that are invasive can metastasize. The most difficult diagnostic task is to differentiate between BCC, SCC, and melanoma noninvasively. SCC appears to contain large amounts of normal cells and has a higher 50 Hz/80 Hz peak ratio, while melanoma has lower 130 Hz/80 Hz peak ratios, as indicated in Figure 7 and Tables 2 and 3. The relationship between the new cells (80 Hz), new blood vessels (130 Hz), and fibrous tissue (260 Hz) provides a means for noninvasively assessing the invasive and metastatic potential of a skin cancers based on the peak ratios of the 50 Hz/80 Hz and 130 Hz/80 Hz ratios.

The ability to predict the invasive potential of skin cancers noninvasively offers potential for early evaluation of lesions that may be difficult to diagnose. Using VOCT, it is possible to image and measure the stiffness of lesions as small as 0.1 mm (see OCT images in Figs. 1–5), which is smaller than can be seen by visual inspection or dermoscopy. VOCT results suggest that new cells (80 Hz peak), new blood vessels (130 Hz peak), and new fibrotic tissue (260 Hz peak) can be used to "fingerprint" cancerous tissues.

It has been reported that an epithelial–mesenchymal transition (EMT) results in a change of the cell phenotype of epidermal cells in epithelial derived cancers and could explain the new cellular peak at 80 Hz. During EMT, epithelial cells lose cell–cell adhesion attachments and reorganize their cytoskeleton. Cell-cell connec-

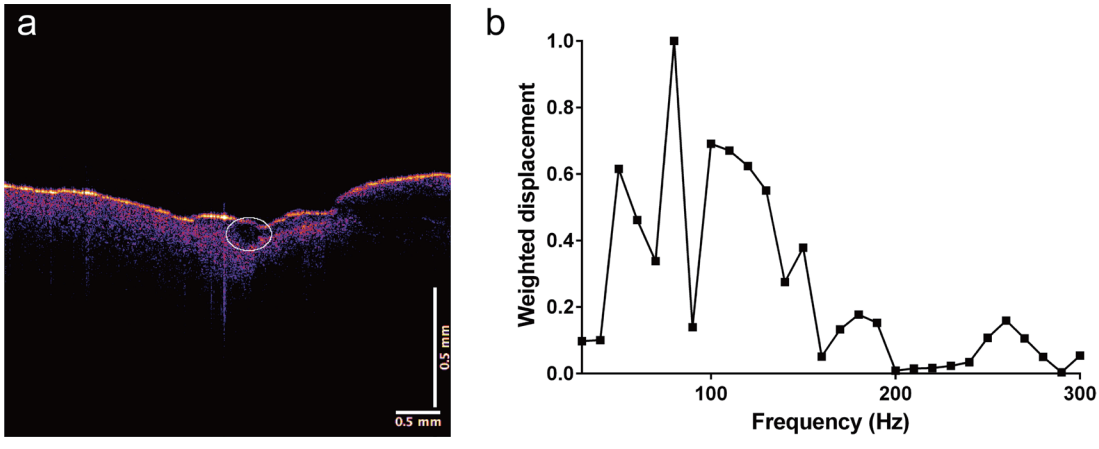

Fig. 5. OCT image and VOCT spectrum form a melanoma. (a) 2D color coded cross-sectional OCT image of a melanoma (circle). (b) Plot of weighted displacement versus frequency showing the mechanovibrational peaks. The increased size of the peaks at 130 Hz and 260 Hz appear to be a characteristic of melanoma as opposed to SCC. The color coding was accomplished by using the pixel intensity and a look-table to assign the colors.

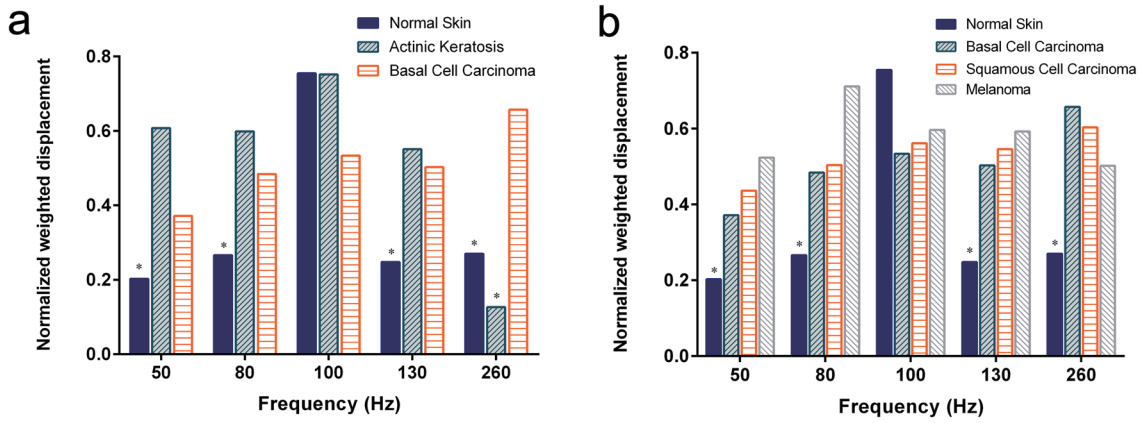

Fig. 6. Bar graph comparing the normalized mechanovibrational peaks seen in the spectra of normal skin, AK, BCC, SCC and melanoma. (a) BCC, SCC, and melanoma. (b) Normal skin, BCC, SCC and melanoma. The peak heights are normalized by dividing by the largest peak in the spectrum. Differences in the 50 Hz, 80 Hz, 130 Hz, and 260 Hz peaks can be used to differentiate between benign and cancerous lesion types and act as a "fingerprint" of each lesion type.

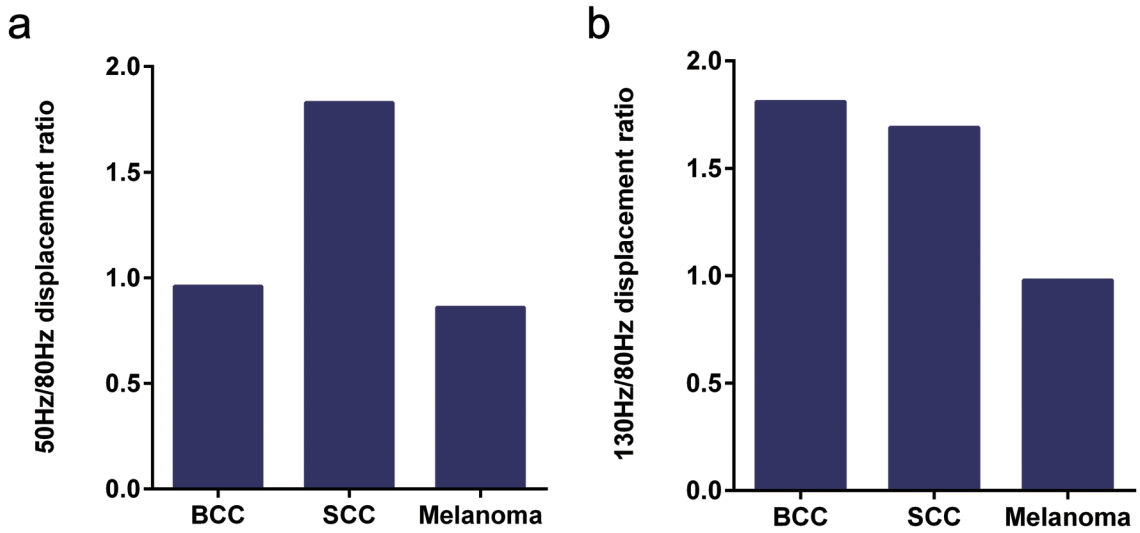

Fig. 7. (a) Bar graph showing the 50 Hz/80 Hz ratio peak heights for BCC, SCC, and melanoma. The increased 50 Hz/80 Hz ratio is significantly different for SCC compared to melanoma and BCC, as shown in Table 2. (b) Bar graph showing the 130 Hz/80 Hz ratio peak heights for BCC, SCC, and melanoma. The decreased 130 Hz/80 Hz ratio is significantly different for melanoma compared to SCC and BCC, as shown in Table 3.

tions loosen, cells become motile, and become resistant to apoptosis.[23] Transforming growth factor beta 1 (TGF-β1), tumor necrosis factor alpha, and hypoxia cooperate to trigger EMT both in cancer and fibrosis,[23,24] converging in the induction of Snail activity through different mechanisms including the activation of transcription factor NF-kB.[24–26] It is possible that the increase in the 80 Hz peak in AK, BCC, SCC, and melanoma is a consequence of EMT, which occurs during normal physiological processes such as wound healing and is not necessarily a marker for cancer since it is reversible.

CAFs become "activated" in tumors through interactions with cancer cells. They can promote tumor progression to malignancy and modify the stromal ECM by enhanced expression and activation of metalloproteinases.[25] The cytokine TGF-β is one of the major prometastatic factors derived from CAFs.[26] Whether the 80 Hz peak includes CAFs is unclear since AK contains a significant 80 Hz peak height. However, since AK is thought to be a pre-can-

Table 2. Peak height ratios and *p*-values for 50 Hz and 80 Hz mechanovibrational peaks for BCC, SCC and melanoma

50 Hz/80 Hz displacement ratios		
	SCC	Melanoma
BCC	0.038[a]	0.37
Melanoma	0.031[a]	

[a]Values show statistical significance.

Table 3. Peak height ratios and *p*-values for 80 Hz and 130 Hz mechanovibrational peaks for BCC, SCC, and melanoma

50 Hz/80 Hz displacement ratios		
	SCC	Melanoma
BCC	0.4	0.045[a]
Melanoma	0.006[a]	

[a]Values show statistical significance.

cerous lesion the 80 Hz peak may be an important diagnostic sign of future formation of skin cancer.

CAFs secrete increased levels of TGF-β,[26–31] which leads to the formation and deposition of dense fibrotic collagen fibers composed mainly of type I collagen (Col I). Col I is another prominent ECM protein with multiple contributions to tumorigenesis[29] and has been reported to promote mammary tumor initiation.[30] A prominent marker of all cancerous lesions studied is the deposition of fibrous collagen peak at 260 Hz with a stiffness of about 16 MPa, which is much higher than about 2.5 MPa reported for the collagen peak at 100 Hz in the dermis.[4–8,20–22]

Inflammatory markers are elaborated by endothelial cells that can sustain or exacerbate the inflammatory process. They recruit and activate leukocytes and have been postulated to lead to EMT transition that also contributes to fibrosis.[31] While the 130 Hz peak is present in AK, BCC, SCC, and melanoma, it is highest in the invasive cancers, SCC, and melanoma, and may indicate a relationship between the appearance of new bloods vessels and invasive potential.

Based on the data in Figures 6 and 7 and Tables 2 and 3, it is possible to noninvasively differentiate among different types of skin cancer. The ability to classify lesions as small as about 0.1 mm in diameter should prove useful in assisting dermatologists in identifying potentially metastatic epithelial cancers and to promote nonsurgical methods to treat early stage benign and possibly malignant lesions. Ongoing studies using quantitative VOCT data in conjunction with machine learning may be useful to rapidly noninvasively identify different skin cancers.

Conclusions

In this study we have shown using VOCT that the morphology and stiffness of benign and cancerous lesions are different based on the addition of new cells with increased stiffness (80 Hz), new blood vessels (130 Hz), and fibrous tissue (260 Hz) present in carcinomas. By normalizing the peaks in the mechanovibrational spectra of the different skin lesions, differences in peak heights and peak ratios (50 Hz/80 Hz and 130 Hz/80 Hz) can be used to differentiate among AK, BCC, SCC, and melanoma and to noninvasively "fingerprint" these different skin lesions. Further studies involving machine learning will provide rapid noninvasive identification of skin lesion "fingerprints" for early screening of cancerous lesions.

It is possible that early diagnosis of small lesions can be enhanced and lead to more extensive use of topical treatments, which may be preferred for benign lesions, as wells as for BCC on the head, face and neck when excision may require extensive additional plastic surgery.

Acknowledgments

The authors would like to thank Dr. Hari Nadiminti and coworkers at Summit Health, Berkeley Heights, NJ, for assistance in collecting the clinical data.

Funding

None.

Conflict of interest

Mr. Tanmay Deshmuhk is an employee of OptoVibronex, LLC. Dr. Frederick H. Silver is a stockholder in OptoVibronex, LLC.

Author contributions

Study concept and design (FHS and TD), performance of experiments (TD), analysis and interpretation of data (FHS), manuscript writing and review (FHS and TD).

Ethical statement

All human studies were reviewed and approved by WCG IRB, approval code 1-1410030-1, 5 April 2021.

Data sharing statement

All data from this study can found at optovobronex.com.

References

[1] Shaw FM, Weinstock MA. Comparing Topical Treatments for Basal Cell Carcinoma. J Invest Dermatol 2018;138(3):484–486. doi:10.1016/j.jid.2017.11.024, PMID:29395168.

[2] Neugebauer R, Su KA, Zhu Z, Sokil M, Chren MM, Friedman GD, *et al*. Comparative effectiveness of treatment of actinic keratosis with topical fluorouracil and imiquimod in the prevention of keratinocyte carcinoma: A cohort study. J Am Acad Dermatol 2019;80(4):998–1005. doi:10.1016/j.jaad.2018.11.024, PMID:30458208.

[3] Halip IA, Vâţă D, Statescu L, Salahoru P, Patraşcu AI, Temelie Olinici D, *et al*. Assessment of Basal Cell Carcinoma Using Dermoscopy and High Frequency Ultrasound Examination. Diagnostics (Basel) 2022;12(3):735. doi:10.3390/diagnostics12030735, PMID:35328289.

[4] Silver FH, Deshmukh T, Benedetto D, Kelkar N. Mechano-vibrational spectroscopy of skin: Are changes in collagen and vascular tissue components early signs of basal cell carcinoma formation? Skin Res Technol 2021;27(2):227–233. doi:10.1111/srt.12921, PMID:32696597.

[5] Silver FH, Kelkar N, Deshmukh T, Ritter K, Ryan N, Nadiminti H. Characterization of the Biomechanical Properties of Skin Using Vibrational Optical Coherence Tomography: Do Changes in the Biomechanical Properties of Skin Stroma Reflect Structural Changes in the Extracellular Matrix of Cancerous Lesions? Biomolecules 2021;11(11):1712. doi:10.3390/biom11111712, PMID:34827711.

[6] Silver FH, Deshmukh T, Kelkar N, Ritter K, Ryan N, Nadiminti H. The "Virtual Biopsy" of Cancerous Lesions in 3D: Non-Invasive Differentiation between Melanoma and Other Lesions Using Vibrational Optical Coherence Tomography. Dermatopathology (Basel) 2021;8(4):539–551. doi:10.3390/dermatopathology8040058, PMID:34940035.

[7] Silver FH, Shah RG, Richard M, Benedetto D. Comparative "virtual biopsies" of normal skin and skin lesions using vibrational optical coherence tomography. Skin Res Technol 2019;25(5):743–749. doi:10.1111/srt.12712, PMID:31127665.

[8] Silver FH, Shah RG, Richard M, Benedetto D. Use of Vibrational Optical Coherence Tomography to Image and Characterize a Squamous Cell Carcinoma. J Dermatology Res Ther 2019;5(1):1–8. doi:10.23937/2469-5750/1510067.

[9] Erdogan B, Webb DJ. Cancer-associated fibroblasts modulate growth factor signaling and extracellular matrix remodeling to regulate tumor metastasis. Biochem Soc Trans 2017;45(1):229–236. doi:10.1042/BST20160387, PMID:28202677.

[10] Yamauchi M, Barker TH, Gibbons DL, Kurie JM. The fibrotic tumor stroma. J Clin Invest 2018;128(1):16–25. doi:10.1172/JCI93554, PMID:29293090.

[11] Cox TR, Bird D, Baker AM, Barker HE, Ho MW, Lang G, *et al*. LOX-mediated collagen crosslinking is responsible for fibrosis-enhanced metastasis. Cancer Res 2013;73(6):1721–1732. doi:10.1158/0008-5472.CAN-12-2233, PMID:23345161.

[12] Park JS, Lee JH, Lee YS, Kim JK, Dong SM, Yoon DS. Emerging role of LOXL2 in the promotion of pancreas cancer metastasis. Oncotarget 2016;7(27):42539–42552. doi:10.18632/oncotarget.9918, PMID:27285767.

[13] Cox TR, Erler JT. Molecular pathways: connecting fibrosis and solid tumor metastasis. Clin Cancer Res 2014;20(14):3637–3643. doi:10.1158/1078-0432.CCR-13-1059, PMID:25028505.
[14] Brücher BL, Jamall IS. Epistemology of the origin of cancer: a new paradigm. BMC Cancer 2014;14:331. doi:10.1186/1471-2407-14-331, PMID:24885752.
[15] Mishra DK, Compean SD, Thrall MJ, Liu X, Massarelli E, Kurie JM, *et al*. Human Lung Fibroblasts Inhibit Non-Small Cell Lung Cancer Metastasis in Ex Vivo 4D Model. Ann Thorac Surg 2015;100(4):1167–74. doi:10.1016/j.athoracsur.2015.05.014, PMID:26233278.
[16] Lallas A, Apalla Z, Argenziano G, Longo C, Moscarella E, Specchio F, *et al*. The dermatoscopic universe of basal cell carcinoma. Dermatol Pract Concept 2014;4(3):11–24. doi:10.5826/dpc.040302, PMID:25126452.
[17] Samani A, Zubovits J, Plewes D. Elastic moduli of normal and pathological human breast tissues: an inversion-technique-based investigation of 169 samples. Phys Med Biol 2007;52(6):1565–1576. doi:10.188/0031-9155/52/6/002, PMID:17327649.
[18] Acerbi I, Cassereau L, Dean I, Shi Q, Au A, Park C, *et al*. Human breast cancer invasion and aggression correlates with ECM stiffening and immune cell infiltration. Integr Biol (Camb) 2015;7(10):1120–1134. doi:10.1039/c5ib00040h, PMID:25959051.
[19] Lin HH, Lin HK, Lin IH, Chiou YW, Chen HW, Liu CY, *et al*. Mechanical phenotype of cancer cells: cell softening and loss of stiffness sensing. Oncotarget 2015;6(25):20946–20958. doi:10.18632/oncotarget.4173, PMID:26189182.
[20] Lekka M. Discrimination Between Normal and Cancerous Cells Using AFM. Bionanoscience 2016;6:65–80. doi:10.1007/s12668-016-0191-3, PMID:27014560.
[21] Silver FH, Kelkar N, Desmukh T. Horvath I, Shah RG. Mechano-Vibrational Spectroscopy of Tissues and Materials Using Vibrational Optical Coherence Tomography: A New Non-Invasive and Non-Destructive Technique. Recent Progress in Materials 2020;2(2):010. doi: 10.21926/rpm.2002010.
[22] Silver FH, Kelkar N, Deshmukh T, Ritter K, Ryan N, Nadiminiti H. Characterization of the biomechanical properties of skin using vibrational optical coherence tomography: Do changes in the biomechanical properties of skin stroma reflect structural changes in the extracellular matrix of cancerous lesions? Biomolecules 2021;11(11):1712. doi:10.3390/biom11111712, PMID:34827711.
[23] Runyan RB, Savagner P. Epithelial-mesenchymal transition and plasticity in the developmental basis of cancer and fibrosis. Dev Dyn 2018;247(3):330–331. doi:10.1002/DVDY.24620, PMID:29446197.
[24] López-Novoa JM, Nieto MA. Inflammation and EMT: an alliance towards organ fibrosis and cancer progression. EMBO Mol Med 2009;1(6-7):303–314. doi:10.1001/emmm200900043, PMID:20049734.
[25] Miles FL, Sikes RA. Insidious changes in stromal matrix fuel cancer progression. Mol Cancer Res 2014;12(3):297–312. doi:10.1158/1541-7786.MCR-13-0535, PMID:24452359.
[26] Yu Y, Xiao CH, Tan LD, Wang QS, Li XQ, Feng YM. Cancer-associated fibroblasts induce epithelial-mesenchymal transition of breast cancer cells through paracrine TGF-β signalling. Br J Cancer 2014;110(3):724–732. doi:10.1038/bjc.2013.768, PMID:24335925.
[27] Ao M, Franco OE, Park D, Raman D, Williams K, Hayward SW. Cross-talk between paracrine-acting cytokine and chemokine pathways promotes malignancy in benign human prostatic epithelium. Cancer Res 2007;67(9):4244–4253. doi:10.1158/0008-5472.CAN-06-3946, PMID:17483336.
[28] Kalluri R, Weinberg RA. The basics of epithelial-mesenchymal transition. J Clin Invest 2009;119(6):1420–1428. doi:10.1172/JCI39104, PMID:19487818.
[29] Levental KR, Yu H, Kass L, Lakins JN, Egeblad M, Erler JT, *et al*. Matrix crosslinking forces tumor progression by enhancing integrin signaling. Cell 2009;139(5):891–906. doi:10.1016/j.cell.2009.10.027, PMID:19931152.
[30] Provenzano PP, Inman DR, Eliceiri KW, Knittel JG, Yan L, Rueden CT, *et al*. Collagen density promotes mammary tumor initiation and progression. BMC Med 2008;6:11. doi:10.1186/1741-7015-6-11, PMID:18442412.
[31] Hsu T, Nguyen-Tran HH, Trojanowska M. Active roles of dysfunctional vascular endothelium in fibrosis and cancer. J Biomed Sci 2019;26(1):86. doi:10.1186/s12929-019-0580-3, PMID:31656195.